

**PROMA PLASMIDS ARE INSTRUMENTAL IN THE DISSEMINATION OF  
LINURON CATABOLIC GENES BETWEEN DIFFERENT GENERA**

**Johannes Werner<sup>1</sup>, Eman Nour<sup>2</sup>, Boyke Bunk<sup>3</sup>, Cathrin Spröer<sup>4</sup>, Kornelia Smalla<sup>2</sup>, Dirk Springael<sup>5</sup>, Başak Öztürk<sup>5,6</sup>**

1 Department of Biological Oceanography, Leibniz Institute for Baltic Sea Research, Rostock, Germany

2 Institute for Epidemiology and Pathogen Diagnostics, Julius Kühn-Institut, Federal Research Centre for Cultivated Plants (JKI), Braunschweig, Germany

3 Bioinformatics Department, Leibniz Institute DSMZ, German Collection of Microorganisms and Cell Cultures, Braunschweig, Germany

4 Central Services, Leibniz Institute DSMZ, German Collection of Microorganisms and Cell Cultures, Braunschweig, Germany

5 Division of Soil and Water Management, KU Leuven, Leuven, Belgium

6 Junior Research Group Microbial Biotechnology, Leibniz Institute DSMZ, German Collection of Microorganisms and Cell Cultures, Braunschweig, Germany

Correspondence Basak Öztürk, Junior Research Group Microbial Biotechnology, Leibniz Institute DSMZ, German Collection of Microorganisms and Cell Cultures, Braunschweig, Germany

Email: [basak.oeztuerk@dsmz.de](mailto:basak.oeztuerk@dsmz.de)

**Running Head: Linuron degradation mediated by PromA plasmids**

Keywords: Broad-host-range plasmids, horizontal gene transfer, biodegradation, transposases, plasmid ecology.

## 28 ABSTRACT

29 PromA plasmids are broad host range plasmids, which are often cryptic and hence  
30 have an uncertain ecological role. We present three novel PromA  $\gamma$  plasmids which  
31 carry genes associated with degradation of the phenylurea herbicide linuron, two  
32 (pPBL-H3-2 and pBPS33-2) of which originate from unrelated *Hydrogenophaga*  
33 hosts isolated from different environments, and one (pEN1) which was  
34 exogenously captured from an on-farm biopurification system. Both  
35 *Hydrogenophaga* plasmids carry all three necessary gene clusters determining the  
36 three main steps for conversion of linuron to Krebs cycle intermediates, while  
37 pEN1 only determines the initial linuron hydrolysis step. Linuron catabolic gene  
38 clusters that determine the same step were identical on all plasmids, encompassed  
39 in differently arranged constellations and characterized by the presence of multiple  
40 *IS1071* elements. In all plasmids except pEN1, the insertion spot of the catabolic  
41 genes in the PromA  $\gamma$  plasmids was the same. Highly similar PromA plasmids  
42 carrying the linuron degrading gene cargo at the same insertion spot were were  
43 previously identified in linuron degrading *Variovorax* sp. Interestingly, in both  
44 *Hydrogenophaga* populations not every PromA plasmid copy carries catabolic  
45 genes. The results indicate that PromA plasmids are important vehicles of linuron  
46 catabolic gene dissemination, rather than being cryptic and only important for the  
47 mobilization of other plasmids.

48

49

## 1 | INTRODUCTION

51 Plasmids are circular or linear extrachromosomal elements that can self-  
52 replicate, and are important agents in the dissemination of genes among microbial  
53 species (Garcillan-Barcia et al., 2011). Broad host range (BHR) plasmids can  
54 independently transfer and maintain themselves in different taxa (Jain and  
55 Srivastava, 2013) and carry accordingly genes for replication, maintenance and  
56 control, and conjugation (Szpirer et al., 1999). In addition, BHR plasmids may carry  
57 so-called "accessory" genes, for instance for antibiotic and heavy metal resistance, or  
58 biodegradation of xenobiotic compounds (Schluter et al., 2007; Sen et al., 2011). On  
59 the other hand, exogenous plasmid capture enabled the isolation of several plasmids  
60 with few or no apparent accessory genes that belong to known BHR plasmid groups  
61 such as IncP-1, IncN and IncU from environmental microbial communities (Brown et  
62 al., 2013). These so far cryptic plasmids have no apparent benefit to the host and are  
63 still propagated in absence of selective pressure (Fox et al., 2008). A recently  
64 discovered group of BHR plasmids are the PromA plasmids, most of which were  
65 isolated by exogenous plasmid capture (Thomas et al., 2017; Van der Auwera et al.,  
66 2009; Schneiker et al., 2001; Yanagiya et al., 2018; Li et al., 2014; Tauch et al., 2002)  
67 hence from unknown hosts, but also few derived from Proteobacterial isolates (Mela et  
68 al., 2008; Ito and Iizuka, 1971; Van der Auwera et al., 2009). With the exception of  
69 SFA231 (Li et al., 2014), pMOL98 (Van der Auwera et al., 2009) and pSB102  
70 (Schneiker et al., 2001) which carry heavy metal resistance-related genes, all 12  
71 completely sequenced PromA plasmids identified to date are cryptic plasmids with

72 no clear indication of their ecological or possible benefit for the host organism. It was  
73 hypothesized that the main role of these plasmids is to mobilize other plasmids  
74 (Zhang et al., 2015).

75 Recently, we have described two PromA plasmids, pPBL-H6-2 and pPBS-H4-2  
76 from two *Variovorax* strains with the metabolic capability to degrade the  
77 phenylurea herbicide linuron (Öztürk et al., 2019). *Variovorax* is a species that is  
78 isolated at high frequency from enrichments aiming for linuron degrading  
79 microorganisms. In the linuron-degrading *Variovorax* species isolated to date, the  
80 initial step of linuron degradation to 3,4-dichloroaniline (DCA) is performed by the  
81 linuron amidases *hyla* or *libA*, followed by the conversion of DCA to 4,5-  
82 dichlorocatechol by the *dcaQAIA2BR* catabolic cluster. The catechol intermediate  
83 is further degraded to Krebs cycle intermediates by the enzymes encoded by the  
84 *ccdCFDER* gene cluster (Bers et al. 2011, 2013). The two *Variovorax* PromA  
85 plasmids belong to the PromA  $\gamma$  subgroup together with the plasmids pSN1104-11  
86 and pSN1104-34 (Yanagiya et al., 2018) that were exogeneously isolated from cow  
87 manure. pPBS-H4-2 is the first PromA plasmid that carries catabolic genes, i.e., it  
88 carries a stretch of DNA containing several gene clusters involved in the  
89 degradation of linuron and several *IS1071* elements, of which two border the cargo  
90 at both ends. In contrast, pPBL-H6-2 only contains one *IS1071* transposase as  
91 cargo.

92 In this study, we report on the characterization of three other linuron catabolic  
93 PromA  $\gamma$  plasmids. In contrast to pPBL-H6-2 and pPBS-H4-2, these plasmids did

94 not originate from *Variovorax*. Two of the new plasmids were isolated from two  
95 different linuron degrading *Hydrogenophaga* strains, PBL-H3 and BPS33.  
96 *Hydrogenophaga* sp. strain PBL-H3 was isolated from a potato field near Halen,  
97 Belgium (Breugelmans et al., 2007) and *Hydrogenophaga* sp. strain BPS33 from  
98 the matrix of an on farm biopurification system (BPS) operated by Inagro, near  
99 Roeselare, Belgium, in this study. *Hydrogenophaga* is not a genus that is frequently  
100 associated with xenobiotic degradation. Exceptions comprise *Hydrogenophaga*  
101 *intermedia* S1 and PMC, which mineralize 4-aminobenzenesulfonate in two-species  
102 consortia (Gan et al., 2011), pyrene-degrading *Hydrogenophaga* sp. PYR1 (Yan et  
103 al., 2017) and 3-/4- hydroxybenzoate-degrading *Hydrogenophaga* sp. H7 (Fan et  
104 al., 2019). The third new PromA plasmid is plasmid pEN1, which was obtained by  
105 biparental exogenous isolation from a BPS operating on a farm near Kortrijk,  
106 Belgium (Dealtry et al., 2016), selecting for mercury resistant exconjugants of the  
107 recipient strain. We compared the full sequences of three new plasmids with each  
108 other and with other previously reported PromA plasmids including those  
109 discovered in the linuron degrading *Variovorax* in order to deduce their evolution  
110 and the role that PromA plasmids play in the dissemination of linuron degradation  
111 genes in different genera and environments.

## 112 2 | MATERIALS AND METHODS

### 113 2.1 | Chemicals

114 Linuron ([3-(3,4-dichlorophenyl)-1-methoxy-1-methyl urea] PESTANAL®,  
115 analytical standard) was purchased from Sigma Aldrich. [phenyl-U-14C] Linuron

116 (16.93 mCi mmol<sup>-1</sup>, radio- chemical purity > 95%) was purchased from Izotop.

## 117 **2.2 | Isolation of *Hydrogenophaga* sp. BPS33**

118 BPS33 was isolated from the matrix of a BPS located on the property of the  
119 research institute Inagro in Rumbeke-Beitem, Belgium (50°54'07.9"N  
120 3°07'28.2"E). The BPS had received linuron and other pesticides for two years.  
121 The sample was collected from the upper 10 cm of the top container, and stored at  
122 4°C until further use. The isolation procedure followed the protocol previously  
123 described by Breugelmans et al. (2007). Briefly, 1 g of the matrix material was  
124 inoculated into 50 ml MMO medium (Dejonghe et al., 2003) containing 20 mg/L  
125 linuron. Degradation of linuron was monitored using HPLC as described before  
126 (Horemans et al., 2014). After linuron was degraded, dilutions of the enrichment  
127 culture were plated on R2A medium (Breugelmans et al., 2007) containing 20 mg/L  
128 linuron. Resulting colonies were inoculated into 2.5 ml 96-well plates containing  
129 500 µL of MMO with 20 mg/L linuron, and colonies that degraded linuron were  
130 identified via 16S rRNA gene sequencing with primers 27F and 1492R (Primers listed  
131 in Table S2). Both BPS33 and PBL-H3 used in this study were routinely cultivated  
132 in R2B supplemented with 20 mg/L linuron. Prior to genome sequencing, the  
133 mineralization capacity of both cultures was determined as described before  
134 (Breugelmans et al., 2007). Each mineralization test contained 10<sup>8</sup> colony forming  
135 units of BPS33 or PBL-H3 in 40 ml MMO and a total radioactivity of 0.009 mCi mL<sup>-1</sup>.  
136 .

### 2.3 | Isolation of pEN1 by exogenous capture

Plasmid pEN1 was exogenously captured from a biopurification system material (Kortrijk, Belgium) spiked with linuron in a microcosm experiment (Dealtry et al., 2016). In brief, *Pseudomonas putida* KT2442 :*gfp* was used as a recipient strain for plasmids conferring mercury chloride resistance (20 µg mL<sup>-1</sup>). Biparental mating was performed with a bacterial suspension extracted from the matrix 25 day after linuron spiking.

### 2.4 | Genome sequencing

DNA was isolated using Qiagen Genomic-tip 100/G (Qiagen, Hilden Germany) according to the instructions of the manufacturer. SMRTbell™ template library was prepared according to the instructions from PacificBiosciences, Menlo Park, CA, USA, following the Procedure & Checklist – Greater Than 10 kbp Template Preparation. Briefly, for preparation of 15 kbp libraries 8 µg genomic DNA and 1.4 µg plasmid DNA was sheared using g-tubes™ from Covaris, Woburn, MA, USA, according to the manufacturer's instructions. DNA was end-repaired and ligated overnight to hairpin adapters applying components from the DNA/Polymerase Binding Kit P6 from Pacific Biosciences, Menlo Park, CA, USA. Reactions were carried out according to the manufacturer's instructions. For the bacterial DNAs BluePippin™ Size-Selection to greater than 4 kbp was performed according to the manufacturer's instructions (Sage Science, Beverly, MA, USA). Conditions for annealing of sequencing primers and binding of polymerase to purified SMRTbell™ template were assessed with the Calculator in RS Remote, PacificBiosciences, Menlo

159 Park, CA, USA. 1 SMRT cell was sequenced per strain/plasmid on the PacBio RSII  
160 (PacificBiosciences, Menlo Park, CA, USA) taking one 240-minutes movies.

161 For the bacterial DNA libraries for sequencing on Illumina platform were  
162 prepared applying Nextera XT DNA Library Preparation Kit (Illumina, San Diego,  
163 USA) with small modifications (Baym et al., 2015). Samples were sequenced on  
164 NextSeq™ 500.

165 Bacterial long read genome assemblies were performed applying the  
166 RS\_HGAP\_Assembly.3 protocol included in SMRT Portal version 2.3.0 applying  
167 target genome sizes of 10 Mbp. For BPS33, the genome assembly directly revealed the  
168 chromosomal and both plasmid sequences. In case of PBL-H3, the assembly revealed  
169 the chromosomal sequence misassembled together with the 107 kbp plasmid. Thus,  
170 this plasmid sequence was separated from the chromosome and processed  
171 independently. Nevertheless, the 319 kbp plasmid was detected as separate contig.  
172 Further artificial contigs constituting of low coverage and/or included in other  
173 replicons were removed from the assembly. All remaining contigs were  
174 circularized; particularly assembly redundancies at the ends of the contigs were  
175 removed. Replicons were adjusted to *dnaA* (chromosome) or *repA-parA* (all  
176 plasmids) as the first gene. Error-correction was performed by a mapping of the  
177 Illumina short reads onto finished genomes using bwa v. 0.6.2 in paired-end  
178 (sampe) mode using default setting (Li and Durbin, 2009) with subsequent variant  
179 and consensus calling using VarScan v. 2.3.6 (Parameters: mpileup2cns –min-  
180 coverage 10 –min-reads2 6 –min-avg-qual 20 –min-var-freq 0.8 –min-freq-for-hom



181 0.75 -p-value 0.01 -strand-filter 1 -variants 1 -output-vcf 1) (Koboldt et al., 2012).

182 A consensus concordance of QV60 could be reached. Automated genome  
183 annotation was carried out using Prokka v. 1.8 (Seemann, 2014). The *hylA*-  
184 containing plasmid was assembled using a target genome size of 200 kbp. However,  
185 only 25 percent of the plasmid population was shown to carry the transposon-based  
186 insertion based on plasmid coverage analysis coverage.

## 187 2.5 | Assembly of pPBL-H3-2 variants B2 and B4

188 The pPBL-H3-2 variants were assembled using the pBPS33-2 as a scaffold. The  
189 PBL-H3 Illumina paired-end reads were mapped to pBPS33-2 using BWA-MEM v.  
190 0.7.17.1 with standard settings (Li and Durbin, 2009) implemented in the Galaxy  
191 platform (Afgan et al., 2016). A consensus of the *dca* cluster genes together with the  
192 flanking regions was generated using samtools v. 2.1.4 mpileup with standard  
193 settings (Li et al., 2009). This consensus was aligned to pPBL-H3-2 (B2). The  
194 flanking regions matched pPBL-H3-2 (B2) perfectly, with *hylA* and the associated  
195 genes being located between these flanking sequences instead of the *dca* cluster. The  
196 consensus sequence with the *dca* cluster, acquired from the mpileup was inserted in  
197 the place of the *hylA* cluster in pPBL-H3-2 (B2) to obtain pPBL-H3-2 (B4). The new  
198 plasmid was annotated as described before. The assembly procedure is illustrated in  
199 Figure S2.

## 200 2.6 | Comparative genomics analysis

201 Both phylogenetic trees and dDDH values were computed on the Type (Strain)  
202 Genome Server (TYGS) (Meier-Kolthoff and Goker, 2019). In brief, the TYGS

203 analysis was subdivided into the following steps: The 16S rRNA gene sequences  
204 were extracted from the genomes using RNAmmer (Lagesen et al., 2007). All  
205 pairwise comparisons among the set of genomes were conducted using GBDP and  
206 intergenomic distances inferred under the algorithm 'trimming' and distance formula  
207  $d_5$  (Meier-Kolthoff et al., 2013). Hundred distance replicates were calculated.  
208 Digital DDH values and confidence intervals were calculated using the  
209 recommended settings of the GGDC 2.1 (Meier-Kolthoff et al., 2013). The resulting  
210 intergenomic distances were used to infer a balanced minimum evolution tree with  
211 branch support via FASTME 2.1.4 including SPR postprocessing (Lefort et al.,  
212 2015). Branch support was inferred from 100 pseudo-bootstrap replicates each. The  
213 trees were rooted at the midpoint and visualized with iTOL (Letunic and Bork,  
214 2019). For constructing the phylogenetic trees, six type strains and six additional  
215 *Hydrogenophaga* genomes were used to determine the phylogenetic position of the  
216 two linuron-degrading *Hydrogenophaga* strains within the genus. A dDDH species  
217 cutoff of 70% was applied as described before (Liu et al., 2015). The list of genomes  
218 included in the study is given in Supplementary table S1.

219 The alignment of the PromA plasmids was performed with AliTV v. 1.0.6  
220 (Ankenbrand et al., 2017). Codon usage frequencies were calculated with Comparem  
221 v 0.0.23 (Parks, 2018), the PCA with R v. 3.5.2 (R Core Team, 2019) and FactoMineR  
222 v. 1.41 (Lê et al., 2008).

223 The plasmid sequences were categorized under known plasmid groups based on  
224 the aa and nucleotide identity of their backbone genes to known plasmids, using

225 BLAST against the NCBI nr database (Altschul et al., 1990). To elucidate the RepA  
226 gene-based phylogeny of the PromA plasmids, nucleotide sequences were aligned  
227 with MUSCLE v. 3.8.31 (Madeira et al., 2019; Edgar, 2004) and the maximum  
228 likelihood (ML) trees were calculated with RaxML v. 8 (Stamatakis, 2014) using the  
229 under the GTR+GAMMA model and 1000 bootstrap replicates. The genomic  
230 locations of the *IS1071* elements and catabolic genes were determined and the genes  
231 were visualized using Geneious v. 11.0.4.

## 232 2.7 | Quantification of bacteria, plasmids and catabolic genes by real-time 233 quantitative PCR (qPCR)

234 The PCR-qPCR primer sequences used in this study are listed in Supplementary  
235 table S2. For the qPCR analysis, the strains BPS33 and PBL-H3 were grown to  
236 OD<sub>600</sub> as described above. DNA extraction was made from 2 ml of culture as  
237 previously-described (Larsen et al., 2007). Each reaction contained 10 ng of template  
238 DNA. qPCR reactions were performed with the ABsolute QPCR Mix (Thermo  
239 Fisher) on a Roche LightCycler 480 II. The qPCRs for 16S rRNA gene (Lopez-  
240 Gutierrez et al., 2004), *hlyA* (Horemans et al., 2016) and *dcaQ* (Albers et al., 2018)  
241 quantification were performed as previously described. qPCR targeting *korB* was  
242 performed as previously-described, except that the Taqman probe was omitted  
243 (Jechalke et al., 2013). Each PCR reaction to generate the templates for the qPCR  
244 standard curves contained 10 ng template DNA (BPS33 gDNA), 1x Dream Taq  
245 Green buffer (Thermo Fisher), 0.2 M of each dNTP, 0.1 μM of each primer and 1.25

246 U of Dream Taq DNA polymerase (Thermo Fisher) in a final volume of 50  $\mu$ l. The  
247 amplification was performed as follows: Initial denaturation of 95°C for 3 min, 40  
248 cycles of denaturation at 95°C for 30 s, annealing at 60°C for 30 s, extension at 72°C  
249 for 1 min, followed by a final extension at 72°C for 15 min. All conventional PCR  
250 reactions were performed with an Applied Biosystems Veriti 96-well thermal  
251 cycler. The products were purified with the DNA Clean&Concentrator 25 kit (Zymo)  
252 and quantified with the Qubit BR DNA assay (Thermo Fisher).

### 253 **3 | RESULTS**

#### 254 **3.1 | Phylogenetic analysis of the PromA plasmids**

255 *Hydrogenophaga* plasmids pPBL-H3-2, pBPS33-2 and exogenously-captured  
256 pEN1, were completely sequenced. The general features of plasmids pEN1, pPBL-  
257 H3-2 and pBPS-33 are given in Table 1.

258 **(Table 1 here)**

259 A whole-sequence alignment revealed that the plasmids pEN1, pBPS-33-2 and  
260 pPBL-H3-2 are very closely related to the previously-described plasmids pPBS-H4-2  
261 and pPBL-H6-2 from linuron-degrading *Variovorax* sp. (Öztürk et al., 2019) (Figure  
262 1). Indeed, RepA-based phylogenetic analysis showed that these plasmids all belong  
263 to the PromA  $\gamma$  group, together with the plasmids pSN1104-11 and pSN1104-34  
264 (Yanagiya et al., 2018) (Figure 2).

265 **(Figure 1 here)**

266 **(Figure 2 here)**

267

268 The RepA sequences, as well as the type IV secretion system sequences of the  
269 PromA  $\gamma$  plasmids were highly-conserved, with 99% identity to each other on amino

270 acid level. Codon usage-based clustering showed that catabolic PromA  $\gamma$  plasmids  
271 clustered together and separately from the non-catabolic ones (Figure 3).

272 **(Figure 3 here)**  
273

### 274 3.2 | Catabolic potential of the PromA plasmids

275 The newly-sequenced PromA plasmids pBPS33-2, pPBL-H3-2 and pEN1 all carry  
276 genes related to linuron-degradation. After the assembly of the PBL-H3 genome, it  
277 was observed that the genome did not contain the *dca* cluster, which was not expected  
278 due to the capacity of this strain to mineralize linuron completely. A BLAST search  
279 against the unassembled PacBio reads indeed revealed the presence of the same *dca*  
280 cluster genes as those present on pBPS33-2. The new assembly, which makes use of  
281 the similarity between the two plasmids as described in the methods section, revealed  
282 that PBL-H3 had two different versions of the pPBL-H3-2 within the population,  
283 named as pPBL-H3-2 (B2) and pPBL-H3-2 (B4). Both pPBL-H3-2 (B2) and pPBL-  
284 H3-2 (B4) are identical except that in the catabolic gene cluster the locus carrying  
285 *hyla* gene and associated open reading frames (ORFs), is replaced by the *dca* cluster  
286 gene cluster (Figure 1).

287 pBPS33-2 carries all the genes necessary for linuron degradation, while pEN1  
288 only contains *hyla*. *hyla*, *dcaQA1A2BR* and *ccdCFDER* are 99% identical to those  
289 previously identified in *Variovorax* sp. WDL1 and PBS-H4. The *hyla* gene on all  
290 plasmids truncates a *dcaQ* gene, with the junction being identical to the *hyla-dcaQ*  
291 junction in pPBS-H4-2 (Öztürk et al., 2019). pEN1 on the other hand carries a *hyla*-  
292 *dcaQ* junction identical to that on pWDL1-1, the *Variovorax* sp. WDL1

293 megaplasmid that carries the linuron degradation genes of this bacterium (Albers et al.,  
294 2018; Öztürk et al., 2019). As previously reported for pWDL1-1 and pPBS-H4-2, the  
295 catabolic clusters on the newly-sequenced PromA plasmids are flanked by *IS1071*-  
296 class II insertion elements, forming putative composite transposons. In pBPS33-2, the  
297 *ccd* and *dca* clusters are adjacent to each other, with one *IS1071* in between, amounting  
298 to three IS elements in total. The *IS1071* element associated with *hylA* is separated  
299 from the *dca* and *ccd* and flanked by two additional *IS1071* elements.

300 In addition to the catabolic clusters related to linuron degradation, pBPS33-2  
301 carries an extra *IS1071* element flanking genes that encode for four proteins  
302 putatively involved in the *meta*-pathway of phenol degradation and three putative  
303 multidrug efflux pump proteins, with an intermittent a single copy of an *IS91*-class  
304 transposase, encompassing in total 18 kbp.

### 305 **3.3 | PromA plasmid associated *IS1071* insertion elements and their synteny**

306 The catabolic PromA plasmids have a high number of *IS1071*- elements, some of which  
307 are associated with the catabolic clusters. *IS1071* elements are absent in the non-  
308 catabolic PromA plasmids, with the exception of pPBL-H6-2 (Öztürk et al., 2019). The  
309 *IS1071* element sequences are largely similar to the classical structure (Sota et al., 2006);  
310 except that some elements seem to code for truncated transposase due to a premature stop  
311 codon (Figure 4). pBPS33-2 has six *IS1071* elements, the highest number among all  
312 PromA plasmids described so far, followed by five in pPBS-H4-2, four in pPBL-H3-2,  
313 two in pEN1 and one in pPBL-H6-2.

314 **(Figure 4 here)**

315 The *IS1071* insertion sites among the plasmids pBPS33-2, pPBL-H3-2 and pPBS-  
316 H4-2 are highly conserved, the first insertion site relative to *repA* being adjacent to the  
317 plasmid mobility genes *mobC* and *virD2* and the 3' end of the last *IS1071* element  
318 being flanked by the backbone *trbM* gene (Figure 4). pPBL-H6-2 only has one  
319 *IS1071* transposase with inverted repeats (IR). For pBPS33-2, pPBL-H3-2 (B2/B4)  
320 and pPBS-H4-2, the first insertion site has been subject to multiple transposon  
321 insertion events, where multiple catabolic clusters and other accessory genes have  
322 been inserted consecutively, being only separated by one *IS1071* element including  
323 IRs. Interestingly, some genes that are associated with DNA replication, such as the  
324 genes encoding for the plasmid replication and segregation proteins RepA and RepB  
325 (100% aa identity to WP\_068682750.1 and WP\_068682748.1, respectively),  
326 segregation proteins ParA and ParB (100% aa identity to CDS81791.1 and  
327 WP\_011114060.1, respectively), tyrosine recombinase XerC (100% aa identity to  
328 WP\_068682758.1) and toxin/antitoxin system genes *klcA/dinJ/yafQ* (100% aa  
329 identity to WP\_011114069.1, WP\_011114070.1 and WP\_011114071.1,  
330 respectively), are also flanked by *IS1071* elements. pPBS-H4-2 and pPBL-H3-2  
331 (B2/B4) carry eight DNA replication-related genes flanked by *IS1071* elements,  
332 which are 100% identical to each other on nucleotide level, while pBPS33-2 carries  
333 three of these eight genes, which are identical to their pPBS-H4-2/pPBL-H3-2  
334 counterparts (*parAB* and *kfrA*). The other PromA  $\gamma$  plasmids lack the *IS1071*-  
335 associated DNA-replication related genes as well as the toxin/antitoxin system genes  
336 altogether. On the other hand, all PromA  $\gamma$  plasmids have copies of *parA* and *parB*

337 genes, which are unrelated to those flanked by the *IS1071* elements on the catabolic  
338 plasmids. In addition to these accessory genes, six putative transposases and thirteen  
339 hypothetical proteins were found in the *IS1071*-flanked region in pPBS-H4-2 and  
340 pPBL-H3-2 (B2/B4), which are conserved among those two. Six of them are present in  
341 pBPS33-2, all of which are annotated as hypothetical proteins. These are absent in  
342 the other PromA  $\gamma$  plasmids.

343 The insertion site of the pEN1 *IS1071* element is an exception among the PromA  
344 plasmids. The insertion site of this *IS1071* element, associated with the *hyla* gene and  
345 adjacent ORFs (Albers et al., 2018; Öztürk et al., 2019), lies between the backbone  
346 genes *repB* and *mobA*. This site is located before the first insertion site of the other  
347 catabolic plasmids relative to *repA*, and exists in other PromA  $\gamma$  plasmids, but with  
348 four nucleotide differences. The *repB-mobA* intergenic region on plasmid SN1104-  
349 34, which has no *IS1071* elements, is identical to pPBS-H4-2, pPBL-H3-2 and  
350 pBPS-33-2, except for a single nucleotide. The left IR of the first *IS1071* element on  
351 pEN1 has twelve nucleotide differences to the previously-described *IS1071* left IR  
352 (Sota et al., 2006). The left IR of the second *IS1071* on pEN1, just like all the other  
353 left IRs on the other catabolic PromA plasmids, is identical to what was previously  
354 described (Sota et al., 2007).

355 In pPBL-H3-2 (B2/B4), the *IS1071* element flanking the right side of the *hyla/dca*  
356 catabolic cluster appears to encode a truncated variant of the *IS1071* transposase, which  
357 is not the case in pBPS33-2 and pPBS-H4-2, where both *IS1071* transposases are  
358 intact (Figure 4). On PBL-H3-2 (B2/B4) and pBPS33-2 the *ccd* cluster is adjacent to



359 the *hylA/dca* clusters, with one *IS1071* element in between. The left flanking *IS1071*  
360 transposase of the *ccd* cluster appears truncated in all PromA plasmids at identical  
361 positions. In all cases, truncations were caused by an immature stop codon as a  
362 result of a point mutation. This truncated transposase was not present in the  
363 pWDL1 of *Variovorax* sp. WDL1, where an identical *ccd* cluster to those on pPBL-  
364 H3-2 (B2 and B4), pBPS33-2 and pPBS-H4-2 is located.

### 365 3.4 | PromA plasmid and catabolic gene copy numbers in *Hydrogenophaga*

366 As there were two variants of the pPBL-H3-2 present in the PBL-H3 population,  
367 the question arose whether each version is represented in equal numbers, and how  
368 this compares to the BPS33 population where only one plasmid version could be  
369 assembled. The copy numbers of the genes encoding for KorB, HylA, DcaQ, as well  
370 as 16S rRNA were determined to elucidate both the number of PromA plasmid  
371 copies (*korB*) per cell and the proportions of PromA plasmids that carry the  
372 catabolic genes. Cultures of PBL-H3 and BPS33 contained approximately 10 copies  
373 of the *korB* gene per cell, hence 10 copies of the PromA plasmid per cell. The *hylA*  
374 and *dcaQ* gene copy numbers in both strains were similar, at about one copy per 100  
375 cells, i.e., about one copy per 1000 PromA plasmid copies.

### 376 3.5 | General genome characteristics and phylogeny

377 The general genome characteristics of the two *Hydrogenophaga* strains are  
378 summarized in Table 1. Prior to sequencing, the ability of both strains to mineralize  
379 linuron was confirmed as described in the Materials and Methods section. Both  
380 genomes comprise of one chromosome and two plasmids.

381 To the date of this publication, 22 *Hydrogenophaga* genomes have been deposited  
382 to GenBank, five of which are complete genomes. The complete list of genomes  
383 included in the phylogenetic analysis is given in Table S1. The complete genomes  
384 have a size of 4.39-6.32 Mbp, with GC contents ranging from 61 to 70%. BPS-33  
385 has the largest genome of them with 6.32 Mbp. This is an exceptional size, the  
386 nearest largest *Hydrogenophaga* genome being 5.23 Mbp. Apart from the linuron-  
387 degrading strains sequenced in this study, only *Hydrogenophaga pseudoflava* DSM  
388 1084 (pDSM1084, NZ\_CP037868.1, 45.2 kbp) contains plasmids.

389 Phylogenetic analysis revealed a distant relation of PBL-H3 and BPS33 to each  
390 other (Figure 5). The computed DNA-DNA hybridization of 25.7% confirms that  
391 these two isolates are different species. The isolates do not belong to any type  
392 species.

393 **(Figure 5 here)**

394 Both *Hydrogenophaga* strains carried megaplasmids, pBPS33-1 and pPBL-H3-1,  
395 which could not be assigned to any known plasmid class. The plasmids do not share  
396 any similarity and have no similarity to megaplasmids previously identified in  
397 *Variovorax* (Öztürk et al., 2019) or any other plasmid from *Hydrogenophaga*.

#### 398 **4 | DISCUSSION**

399 In this study, we have investigated the genomic basis of linuron degradation by the  
400 two *Hydrogenophaga* strains PBL-H3 and BPS33, and the role of PromA plasmids  
401 in the dissemination of catabolic genes in different environments. The genomes of

402 two linuron-degrading *Hydrogenophaga* strains were completely sequenced and  
403 chromosomes and plasmids were circularized. These strains were sampled from two  
404 different environments, and although they belong to the same genus, they are  
405 distantly related to each other. The linuron-degrading *Variovorax* strains were very  
406 closely related to each other despite belonging to different species (Öztürk et al.,  
407 2019). Within the *Hydrogenophaga* genus however, the ability to acquire xenobiotic  
408 degradation genes seems to be independent of the host phylogeny.

409 The PromA plasmids pPBL-H3-2 and pBPS33-2 are the sole carriers of linuron-  
410 related catabolic clusters in both strains analyzed in this study. This was also the case  
411 for *Variovorax* sp. PBS-H4, although this strain lacks the *dca* cluster genes that are  
412 required for complete linuron mineralization (Öztürk et al., 2019). Remarkably, the  
413 catabolic PromA plasmids have a near-identical backbone to the previously-  
414 described PromA  $\gamma$  plasmids isolated in Japan (Yanagiya et al., 2018). It has been  
415 reported before that BHR plasmids isolated from different geographic locations can be  
416 highly-conserved (Li et al., 2016; Heuer et al., 2004; Chen et al., 2015b), however,  
417 some degree of divergence in the backbone structures of PromA plasmid groups  
418 were reported before (Li et al., 2014). In this case, the near-identical backbone genes  
419 indicate that these plasmids had a recent common ancestor, probably without any  
420 accessory genes. Interestingly, the PromA plasmids of PBL-H3 (B2) and PBS-H4,  
421 which were isolated from the same soil sample, have a high synteny of their cargo  
422 genes, indicating that these plasmids are variants of each other and can possibly be  
423 transferred within these two genera in the same environment. The codon usage

424 distribution of the closely related PromA  $\gamma$  plasmids differ among those with and  
425 without catabolic clusters, indicating that the cargo genes differ in codon usage  
426 from the backbone genes.

427 *IS1071* elements were associated with all catabolic clusters related to linuron  
428 degradation on all plasmids. Remarkably, all catabolic clusters were near-identical  
429 to what has previously been described for *Variovorax* (Öztürk et al., 2019), both in  
430 terms of gene identity and synteny. This demonstrates that even among different  
431 genera and environments, the linuron-degradation pathways rely on a limited  
432 genetic repertoire, and the role of *IS1071* elements to transfer these genes is not  
433 limited to a certain genus or environment. The cargo associated by *IS1071* elements  
434 on these plasmids, however, were not limited to catabolic genes. Putative plasmid  
435 backbone genes involved in plasmid replication and maintenance as well as  
436 hypothetical proteins were also associated with *IS1071* elements, which were  
437 absent in the PromA plasmids without *IS1071* elements. The nearest relatives of the  
438 plasmid backbone genes associated with *IS1071* elements originated from different  
439 organisms and plasmids, among which are IncP-1 plasmids (*parAB*) but also non-  
440 linuron-degrading *Variovorax* chromosomes (*repAB*). It is worth noting that *IS1071*  
441 type transposases were not the only transposases located on some of the PromA  
442 plasmids. Especially pPBS-H4-2 and pPBL-H3-2 (B2/B4) carry a number of  
443 different transposases, showing that PromA plasmids are prone to acquiring mobile  
444 genetic elements and driving horizontal gene transfer.

445 The identical *IS1071* insertion sites on the PromA  $\gamma$  plasmids indicate hot spots for

446 transposon insertion. Hot spots were previously-reported for IncP plasmids with  
447 *IS1071* elements (Sota et al., 2007; Dunon et al., 2018; Thorsted et al., 1998). The  
448 insertion of transposons at specific sites contributes to plasmid stability (Sota et al.,  
449 2007). The hot spot on our PromA  $\gamma$  plasmids is located between the genes  
450 encoding for the relaxase VirD2 and conjugal transfer protein TrbM, which is  
451 different from the *parA* locus that was previously shown to be the insertion site of  
452 pSFA231 (Li et al., 2014), pMOL98 (Van der Auwera et al., 2009) and pSB102  
453 (Schneiker et al., 2001) as well as using PCR-based methods in metagenomes (Dias  
454 et al., 2018). The PromA  $\gamma$  insertion hot spot is in some cases occupied by multiple  
455 consecutive IS elements. The counterparts of the insertion site on pEN1 on the  
456 other catabolic plasmids on the other hand, are not occupied despite the fact that  
457 these plasmids all carry a high number of *IS1071* elements.

458 The qPCR results indicate that the *hylA* and *dca* cluster carrying PromA plasmids  
459 are underrepresented by almost 100-fold compared to the total number of PromA  
460 plasmids in both species. This holds true for pPBL-H3-2, for which two variants  
461 carrying either *hylA* or *dca* genes were assembled, as well as pBPS33-2. The qPCR  
462 results show that both BPS33 and PBL-H3 populations harbour different PromA  
463 plasmids, of which not all have the *hylA* gene or the *dca* cluster, and the majority  
464 lack both. Isogenic subpopulations carrying either *hylA* or *dca* genes were reported  
465 for *Variovorax* sp. WDL1 before (Albers et al., 2018). It was proposed that the  
466 existence of two subpopulations may be an adaptation to linuron degradation in a  
467 consortium, where linuron is degraded to DCA *hylA*-carrying consortium member, while the

468 DCA degradation is performed by the other consortium members (Albers et al., 2018).  
469 Indeed, PBL-H3 indeed tends to accumulate DCA when growing on linuron on its  
470 own, and performed much better in a consortium with other DCA degraders  
471 (Breugelmans et al., 2007). Thus, *Hydrogenophaga* strains might be adapted in a  
472 similar way. Interestingly, the linuron catabolic genes of both *Hydrogenophaga*  
473 strains are near-identical to those of *Variovorax* strains WDL1 and PBS-H4, where  
474 WDL1 degrades linuron less efficiently on its own than when it is a part of a  
475 consortium (Dejonghe et al. 2003), and PBS-H4 can only perform the conversion of  
476 linuron to DCA (Breugelmans et al. 2007). The major difference between the  
477 *Variovorax* sp. WDL1 and *Hydrogenophaga* subpopulations is that, in WDL1 the  
478 majority of the population has either the *hylA* gene or the *dca* cluster (Albers et al.,  
479 2018), while in both *Hydrogenophaga* strains subpopulations containing either  
480 gene are much underrepresented.

481 The results show that even among different genera, the genes for complete  
482 linuron mineralization are highly- conserved, being acquired through horizontal gene  
483 transfer which is mediated by BHR plasmids. PromA  $\gamma$  plasmids, in addition to the  
484 previously-known IncP-1 plasmids, are carriers of *IS1071* elements and associated  
485 catabolic pathways, being present in different contaminated ecosystems. In contrast to  
486 the linuron-degrading *Variovorax* species, where the degradation genes are also  
487 found on megaplasmids as well as BHR plasmids (Öztürk et al., 2019), the  
488 *Hydrogenophaga* catabolic genes are only found on BHR plasmids, pointing towards  
489 a more recent acquisition of these gene clusters.

#### 4.1 Data availability

The BPS33 genome is available under the accession numbers CP044549-CP044551, PBL-H3 (B2) under CP044975-CP044977, PBL-H3 (B4) under CP044972-CP044974 and pEN1 plasmid sequence under MN536506.

#### ACKNOWLEDGEMENTS

This work was supported by the EU 7th Framework Programme (MetaExplore 222625) and FWO Project G.0371.06. We thank Anja Heuer and Simone Severitt for technical assistance, Charlotte Roschka for her help in sequence analysis and assembly, and Jörg Overmann for his support for sequencing of the strains. Johannes Werner personally acknowledges the use of de.NBI cloud and the support by the High Performance and Cloud Computing Group at the Zentrum für Datenverarbeitung of the University of Tübingen and the Federal Ministry of Education and Research (BMBF) through grant no 031 A535A.

#### AUTHOR CONTRIBUTIONS STATEMENT

BÖ designed the study and performed the experiments on the *Hydrogenophaga* strains. BÖ and JW performed the sequence analysis of the *Hydrogenophaga* genomes and comparative analysis of PromA plasmids. BB and CS performed the sequencing and assembly of all genomes and plasmids. EN and KS isolated pEN1 and performed the sequence analysis. BÖ, JW, and DS wrote the main body of the paper. All authors contributed to the writing and critical reading of this publication.

#### CONFLICT OF INTEREST STATEMENT

512 The authors declare no conflict of interest.



## REFERENCES

- 514 Afgan, E., Baker, D., van den Beek, M., Blankenberg, D., Bouvier, D., Cech, M.,  
515 Chilton, J., Clements, D., Coraor, N., Eberhard, C., Gruning, B., Guerler, A.,  
516 Hillman-Jackson, J., Von Kuster, G., Rasche, E., Soranzo, N., Turaga, N., Taylor, J.,  
517 Nekrutenko, A. and Goecks, J. (2016) The Galaxy platform for accessible,  
518 reproducible and collaborative biomedical analyses: 2016 update. *Nucleic Acids*  
519 *Res.*, **44**, W3–W10.
- 520
- 521 Albers, P., Lood, C., Ozturk, B., Horemans, B., Lavigne, R., van Noort, V., De Mot,  
522 R., Marchal, K., Sanchez-Rodriguez, A. and Springael, D. (2018) Catabolic task  
523 division between two near-isogenic subpopulations co-existing in a herbicide-  
524 degrading bacterial consortium: consequences for the interspecies consortium  
525 metabolic model. *Environ. Microbiol.*, **20**, 85–96.
- 526
- 527 Altschul, S. F., Gish, W., Miller, W., Myers, E. W. and Lipman, D. J. (1990) Basic local  
528 alignment search tool. *J Mol Biol*, **215**, 403 – 410.
- 529
- 530 Ankenbrand, M. J., Hohlfeld, S., Hackl, T. and Förster, F. (2017) AliTV—interactive  
531 visualization of whole genome comparisons. *PeerJ Comp Sci*, **3**, e116.
- 532
- 533 Van der Auwera, G. A., Krol, J. E., Suzuki, H., Foster, B., Van Houdt, R., Brown, C. J.,  
534 Mergeay, M. and Top, E. M. (2009) Plasmids captured in *C. metallidurans* CH34:

535 defining the PromA family of broad-host-range plasmids. *Antonie Van Leeuwenhoek*,  
536 **96**, 193–204.

537

538 Baym, M., Kryazhimskiy, S., Lieberman, T. D., Chung, H., Desai, M. M. and Kishony,  
539 R. (2015) Inexpensive multiplexed library preparation for megabase-sized genomes.  
540 *PLoS ONE*, **10**, e0128036.

541

542 Bers K et al. 2011. A novel hydrolase identified by genomic-proteomic analysis of  
543 phenylurea herbicide mineralization by *Variovorax* sp. strain SRS16. *Appl.*  
544 *Environ. Microbiol.*

545

546 Bers K et al. 2013. Hyla, an alternative hydrolase for initiation of catabolism of the  
547 phenylurea herbicide linuron in *Variovorax* sp. strains. *Appl. Environ. Microbiol.*  
548 **79**:5258–5263.

549

550 Breugelmans, P., D’Huys, P. J., De Mot, R. and Springael, D. (2007) Characterization  
551 of novel linuron-mineralizing bacterial consortia enriched from long-term linuron-  
552 treated agricultural soils. *FEMS Microbiol. Ecol.*, **62**, 374–385.

553

554 Brown, C. J., Sen, D., Yano, H., Bauer, M. L., Rogers, L. M., Van der Auwera, G. A. and  
555 Top, E. M. (2013) Diverse broad-host-range plasmids from freshwater carry few  
556 accessory genes. *Appl. Environ. Microbiol.*, **79**, 7684–7695.

557

558 Chen, J., Bhattacharjee, H. and Rosen, B. P. (2015a) ArsH is an organoarsenical  
559 oxidase that confers resistance to trivalent forms of the herbicide monosodium  
560 methylarsenate and the poultry growth promoter roxarsone. *Mol. Microbiol.*, **96**,  
561 1042– 1052.

562

563 Chen, K., Xu, X., Zhang, L., Gou, Z., Li, S., Freilich, S. and Jiang, J. (2015b) Comparison  
564 of four *Comamonas* catabolic plasmids reveals the Evolution of pBHB To catabolize  
565 haloaromatics. *Appl. Environ. Microbiol.*, **82**, 1401–1411.

566

567 Dealtry, S., Nour, E. H., Holmsgaard, P. N., Ding, G. C., Weichelt, V., Dunon, V., Heuer,  
568 H., Hansen, L. H., Sørensen, S. J., Springael, D. and Smalla, K. (2016) Exploring the  
569 complex response to linuron of bacterial communities from biopurification systems  
570 by means of cultivation-independent methods. *FEMS Microbiol. Ecol.*, **92**.

571

572 Dejonghe, W., Berteloot, E., Goris, J., Boon, N., Crul, K., Maertens, S., Hofte, M., De  
573 Vos, P., Verstraete, W. and Top, E. M. (2003) Synergistic degradation of linuron by a  
574 bacterial consortium and isolation of a single linuron-degrading *Variovorax* strain.  
575 *Appl. Environ. Microbiol.*, **69**, 1532–1541.

576

577 Di Gioia, D., Peel, M., Fava, F. and Wyndham, R. C. (1998) Structures of homologous  
578 composite transposons carrying *cbaABC* genes from Europe and North America.

579 *Appl. Environ. Microbiol.*, **64**, 1940–1946.

580

581 Dias, A. C. F., Cotta, S. R., Andreote, F. D. and van Elsas, J. D. (2018) The *parA* region  
582 of broad-host-range PromA plasmids is a carrier of mobile genes. *Microb. Ecol.*, **75**,  
583 479–486.

584

585 Dunon, V., Bers, K., Lavigne, R., Top, E. M. and Springael, D. (2018) Targeted  
586 metagenomics demonstrates the ecological role of *IS1071* in bacterial community  
587 adaptation to pesticide degradation. *Environ. Microbiol.*, **20**, 4091–4111.

588

589 Dunon, V., Sniegowski, K., Bers, K., Lavigne, R., Smalla, K. and Springael, D. (2013)  
590 High prevalence of IncP-1 plasmids and *IS1071* insertion sequences in on-farm  
591 biopurification systems and other pesticide-polluted environments. *FEMS Microbiol.*  
592 *Ecol.*, **86**, 415–431.

593

594 Edgar, R. C. (2004) MUSCLE: multiple sequence alignment with high accuracy and  
595 high throughput. *Nucleic Acids Res.*, **32**, 1792–1797.

596

597 Fan, X., Nie, L., Shi, K., Wang, Q., Xia, X. and Wang, G. (2019) Simultaneous 3-/4-  
598 hydroxybenzoates biodegradation and arsenite oxidation by *Hydrogenophaga* sp. H7.  
599 *Front Microbiol.*, **10**, 1346.

600

- 601 Fox, R. E., Zhong, X., Krone, S. M. and Top, E. M. (2008) Spatial structure and nutrients  
602 promote invasion of IncP-1 plasmids in bacterial populations. *ISME J*, **2**, 1024–1039.  
603
- 604 Gan, H. M., Shahir, S., Ibrahim, Z. and Yahya, A. (2011) Biodegradation of 4-  
605 aminobenzenesulfonate by *Ralstonia* sp. PBA and *Hydrogenophaga* sp. PBC isolated  
606 from textile wastewater treatment plant. *Chemosphere*, **82**, 507–513.  
607
- 608 Garcillan-Barcia, M. P., Alvarado, A. and de la Cruz, F. (2011) Identification of bacterial  
609 plasmids based on mobility and plasmid population biology. *FEMS Microbiol. Rev.*,  
610 **35**, 936–956.  
611
- 612 Heuer, H., Szczepanowski, R., Schneiker, S., Puhler, A., Top, E. M. and Schluter, A.  
613 (2004) The complete sequences of plasmids pB2 and pB3 provide evidence for a  
614 recent ancestor of the IncP-1 beta group without any accessory genes. *Microbiology*  
615 (*Reading, Engl.*), **150**, 3591–3599.  
616
- 617 Horemans, B., Bers, K., Ruiz Romero, E., Pose Juan, E., Dunon, V., De Mot, R. and  
618 Springael, D. (2016) Functional redundancy of linuron degradation in microbial  
619 communities in agricultural soil and biopurification systems. *Appl. Environ.*  
620 *Microbiol.*, **82**, 2843–2853.  
621
- 622 Horemans, B., Hofkens, J., Smolders, E. and Springael, D. (2014) Biofilm formation of

623 a bacterial consortium on linuron at micropollutant concentrations in continuous flow  
624 chambers and the impact of dissolved organic matter. *FEMS Microbiol. Ecol.*, **88**,  
625 184–194.

626

627 Huerta-Cepas, J., Forslund, K., Coelho, L. P., Szklarczyk, D., Jensen, L. J., von Mering, C.  
628 and Bork, P. (2017) Fast genome-wide functional annotation through orthology  
629 assignment by eggNOG-Mapper. *Mol. Biol. Evol.*, **34**, 2115–2122.

630

631 Ito, H. and Iizuka, H. (1971) Taxonomic studies on a radio-resistant pseudomonas.  
632 *Agricultural and Biological Chemistry*, **35**, 1566–1571.

633 Jain, A. and Srivastava, P. (2013) Broad host range plasmids. *FEMS*  
634 *Microbiol. Lett.*, **348**, 87–96.

635 Jechalke, S., Dealtry, S., Smalla, K. and Heuer, H. (2013) Quantification of IncP-1  
636 plasmid prevalence in environmental samples. *Appl. Environ. Microbiol.*, **79**, 1410–  
637 1413.

638

639 Koboldt, D. C., Zhang, Q., Larson, D. E., Shen, D., McLellan, M. D., Lin, L., Miller, C.  
640 A., Mardis, E. R., Ding, L. and Wilson, R. K. (2012) VarScan 2: somatic mutation  
641 and copy number alteration discovery in cancer by exome sequencing. *Genome Res.*,  
642 **22**, 568–576.

643

644 Lagesen, K., Hallin, P., Rørdland, E. A., Staerfeldt, H. H., Rognes, T. and Ussery, D. W.

- 645 (2007) RNAmmer: consistent and rapid annotation of ribosomal RNA genes.  
646 *Nucleic Acids Res.*, **35**, 3100–3108.
- 647
- 648 Larsen, M. H., Biermann, K., Tandberg, S., Hsu, T. and Jacobs, W. R. (2007) Genetic  
649 manipulation of *Mycobacterium tuberculosis*. *Curr Protoc Microbiol*, **Chapter 10**,  
650 Unit 10A.2.
- 651
- 652 Lefort, V., Desper, R. and Gascuel, O. (2015) FastME 2.0: A Comprehensive, accurate,  
653 and fast distance-based phylogeny inference program. *Mol. Biol. Evol.*, **32**, 2798–  
654 2800.
- 655
- 656 Letunic, I. and Bork, P. (2019) Interactive Tree Of Life (iTOL) v4: recent updates and  
657 new developments. *Nucleic Acids Res.*, **47**, W256–W259.
- 658
- 659 Li, H. and Durbin, R. (2009) Fast and accurate short read alignment with Burrows-  
660 Wheeler transform. *Bioinformatics*, **25**, 1754–1760.
- 661
- 662 Li, H., Handsaker, B., Wysoker, A., Fennell, T., Ruan, J., Homer, N., Marth, G.,  
663 Abecasis, G. and Durbin, R. (2009) The Sequence Alignment/Map format and  
664 SAMtools. *Bioinformatics*, **25**, 2078–2079.
- 665
- 666 Li, X., Top, E. M., Wang, Y., Brown, C. J., Yao, F., Yang, S., Jiang, Y. and Li, H. (2014)

667 The broad-host-range plasmid pSFA231 isolated from petroleum-contaminated  
668 sediment represents a new member of the PromA plasmid family. *Front Microbiol*,  
669 **5**, 777.

670

671 Li, X., Wang, Y., Brown, C. J., Yao, F., Jiang, Y., Top, E. M. and Li, H. (2016)  
672 Diversification of broad host range plasmids correlates with the presence of antibiotic  
673 resistance genes. *FEMS Microbiol. Ecol.*, **92**.

674

675 Liu, Y., Lai, Q., Goker, M., Meier-Kolthoff, J. P., Wang, M., Sun, Y., Wang, L. and  
676 Shao, Z. (2015) Genomic insights into the taxonomic status of the *Bacillus cereus*  
677 group. *Sci Rep*, **5**, 14082.

678

679 Lopez-Gutierrez, J. C., Henry, S., Hallet, S., Martin-Laurent, F., Catroux, G. and  
680 Philippot, L. (2004) Quantification of a novel group of nitrate-reducing bacteria in  
681 the environment by real-time PCR. *J. Microbiol. Methods*, **57**, 399–407.

682

683 Lê, S., Josse, J. and Husson, F. (2008) Factominer: An R package for multivariate  
684 analysis. *J Stat Softw*, **25**, 1–18.

685

686 Madeira, F., Park, Y. M., Lee, J., Buso, N., Gur, T., Madhusoodanan, N., Basutkar, P.,  
687 Tivey, A. R. N., Potter, S. C., Finn, R. D. and Lopez, R. (2019) The EMBL-EBI search  
688 and sequence analysis tools APIs in 2019. *Nucleic Acids Res.*, **47**, W636–W641.



689

690 Martinez, B., Tomkins, J., Wackett, L. P., Wing, R. and Sadowsky, M. J. (2001)  
691 Complete nucleotide sequence and organization of the atrazine catabolic plasmid  
692 pADP-1 from *Pseudomonas* sp. strain ADP. *J. Bacteriol.*, **183**, 5684–5697.

693

694 Martini, M. C., Albicoro, F. J., Nour, E., Schluter, A., van Elsas, J. D., Springael, D.,  
695 Smalla, K., Pistorio, M., Lagares, A. and Del Papa, M. F. (2015) Characterization of a  
696 collection of plasmid-containing bacteria isolated from an on-farm biopurification  
697 system used for pesticide removal. *Plasmid*, **80**, 16–23.

698

699 Martini, M. C., Wibberg, D., Lozano, M., Torres Tejerizo, G., Albicoro, F. J., Jaenicke,  
700 S., van Elsas, J. D., Petroni, A., Garcillan- Barcia, M. P., de la Cruz, F., Schluter, A.,  
701 Puhler, A., Pistorio, M., Lagares, A. and Del Papa, M. F. (2016) Genomics of high  
702 molecular weight plasmids isolated from an on-farm biopurification system. *Sci Rep*,  
703 **6**, 28284.

704

705 Meier-Kolthoff, J. P., Auch, A. F., Klenk, H. P. and Goker, M. (2013) Genome  
706 sequence-based species delimitation with confidence intervals and improved  
707 distance functions. *BMC Bioinformatics*, **14**, 60.

708

709 Meier-Kolthoff, J. P. and Goker, M. (2019) TYGS is an automated high-throughput  
710 platform for state-of-the-art genome-based taxonomy. *Nat Commun*, **10**, 2182.

711

712 Mela, F., Fritsche, K., Boersma, H., van Elsas, J. D., Bartels, D., Meyer, F., de Boer, W.,  
713 van Veen, J. A. and Leveau, J. H. (2008) Comparative genomics of the pIPO2/pSB102  
714 family of environmental plasmids: sequence, evolution, and ecology of pTer331  
715 isolated from *Collimonas fungivorans* Ter331. *FEMS Microbiol. Ecol.*, **66**, 45–62.

716

717 Nies, D. H. (1995) The cobalt, zinc, and cadmium efflux system CzcABC from  
718 *Alcaligenes eutrophus* functions as a cation- proton antiporter in *Escherichia coli*. *J.*  
719 *Bacteriol.*, **177**, 2707–2712.

720

721 Parks, D. (2018) Comparem. <https://github.com/dparks1134/CompareM>.

722

723 R Core Team (2019) *R: A Language and Environment for Statistical Computing*. R  
724 Foundation for Statistical Computing, Vienna, Austria. URL: [https://www.R-](https://www.R-project.org/)  
725 [project.org/](https://www.R-project.org/).

726

727 San Millan, A. and MacLean, R. C. (2017) Fitness Costs of Plasmids: a Limit to  
728 Plasmid Transmission. *Microbiol Spectr*, **5**.

729

730 Schluter, A., Szczepanowski, R., Puhler, A. and Top, E. M. (2007) Genomics of IncP-1  
731 antibiotic resistance plasmids isolated from wastewater treatment plants provides  
732 evidence for a widely accessible drug resistance gene pool. *FEMS Microbiol. Rev.*, **31**,

- 733 449–477.
- 734
- 735 Schneiker, S., Keller, M., Droge, M., Lanka, E., Puhler, A. and Selbitschka, W. (2001)
- 736 The genetic organization and evolution of the broad host range mercury resistance
- 737 plasmid pSB102 isolated from a microbial population residing in the rhizosphere of
- 738 alfalfa. *Nucleic Acids Res.*, **29**, 5169–5181.
- 739
- 740 Seemann, T. (2014) Prokka: rapid prokaryotic genome annotation. *Bioinformatics*,
- 741 **30**, 2068–2069.
- 742
- 743 Sen, D., Van der Auwera, G. A., Rogers, L. M., Thomas, C. M., Brown, C. J. and Top, E.
- 744 M. (2011) Broad-host-range plasmids from agricultural soils have IncP-1 backbones
- 745 with diverse accessory genes. *Appl. Environ. Microbiol.*, **77**, 7975–7983.
- 746
- 747 Sota, M., Tsuda, M., Yano, H., Suzuki, H., Forney, L. J. and Top, E. M. (2007) Region-
- 748 specific insertion of transposons in combination with selection for high plasmid
- 749 transferability and stability accounts for the structural similarity of IncP-1 plasmids.
- 750 *J. Bacteriol.*, **189**, 3091–3098.
- 751
- 752 Sota, M., Yano, H., Nagata, Y., Ohtsubo, Y., Genka, H., Anbutsu, H., Kawasaki, H. and
- 753 Tsuda, M. (2006) Functional analysis of unique class II insertion sequence IS1071.
- 754 *Appl. Environ. Microbiol.*, **72**, 291–297.

755

756 Stamatakis, A. (2014) RAxML version 8: a tool for phylogenetic analysis and post-  
757 analysis of large phylogenies. *Bioinformatics*, **30**, 1312–1313.

758

759 Szpirer, C., Top, E., Couturier, M. and Mergeay, M. (1999) Retrotransfer or gene  
760 capture: a feature of conjugative plasmids, with ecological and evolutionary  
761 significance. *Microbiology (Reading, Engl.)*, **145 ( Pt 12)**, 3321–3329.

762

763 Tauch, A., Schneiker, S., Selbitschka, W., Puhler, A., van Overbeek, L. S., Smalla, K.,  
764 Thomas, C. M., Bailey, M. J., Forney, L. J., Weightman, A., Ceglowski, P.,  
765 Pembroke, T., Tietze, E., Schroder, G., Lanka, E. and van Elsas, J. D. (2002) The  
766 complete nucleotide sequence and environmental distribution of the cryptic,  
767 conjugative, broad-host-range plasmid pIPO2 isolated from bacteria of the wheat  
768 rhizosphere. *Microbiology (Reading, Engl.)*, **148**, 1637–1653.

769

770 Thomas, C. M., Thomson, N. R., Cerdeno-Tarraga, A. M., Brown, C. J., Top, E. M. and  
771 Frost, L. S. (2017) Annotation of plasmid genes. *Plasmid*, **91**, 61–67.

772

773 Vedler, E., Vahter, M. and Heinaru, A. (2004) The completely sequenced plasmid  
774 pEST4011 contains a novel IncP1 backbone and a catabolic transposon harboring *tfd*  
775 genes for 2,4-dichlorophenoxyacetic acid degradation. *J. Bacteriol.*, **186**, 7161–  
776 7174.

- 777 Thorsted, P. B., Shah, D. S., Macartney, D., Kostelidou, K. and Thomas, C. M. (1996)  
778 Conservation of the genetic switch between replication and transfer genes of IncP  
779 plasmids but divergence of the replication functions which are major host-range  
780 determinants. *Plasmid*, **36**, 95–111.
- 781
- 782 Yan, Z., Zhang, Y., Wu, H., Yang, M., Zhang, H., Hao, Z. and Jiang, H. (2017) Isolation  
783 and characterization of a bacterial strain *Hydrogenophaga* sp. pyr1 for anaerobic  
784 pyrene and benzo[a]pyrene biodegradation. *RSC Adv.*, **7**, 46690–46698.
- 785
- 786 Yanagiya, K., Maejima, Y., Nakata, H., Tokuda, M., Moriuchi, R., Dohra, H., Inoue,  
787 K., Ohkuma, M., Kimbara, K. and Shintani, M. (2018) Novel self-transmissible and  
788 broad-host-range plasmids exogenously captured from anaerobic granules or cow  
789 manure. *Front Microbiol.*, **9**, 2602.
- 790
- 791 Zhang, M., Visser, S., Pereira e Silva, M. C. and van Elsas, J. D. (2015) IncP-1 and  
792 PromA group plasmids are major providers of horizontal gene transfer capacities  
793 across bacteria in the mycosphere of different soil fungi. *Microb. Ecol.*, **69**, 169–179.
- 794
- 795 Öztürk, B., Werner, J., Meier-Kolthoff, J. P., Bunk, Spröer, C. and Springael, D. (2019)  
796 Comparative genomics unravels mechanisms of genetic adaptation for the catabolism  
797 of the phenylurea herbicide linuron in *Variovorax*. *bioRxiv* 759100; doi:  
798 <https://doi.org/10.1101/759100>

799 5 | **Figure Captions**

800 **FIGURE 1** Alignment of PromA  $\gamma$  plasmids. Alignment identities are shown for  
801 an identity of 90-100%. Each plasmid is aligned to the one above.

802 **FIGURE 2** *repA* gene-based phylogeny of PromA plasmids. The branches are  
803 scaled in terms of the expected number of substitutions per site. The numbers above  
804 the branches are support values when larger than 60 % from ML.

805 **FIGURE 3** PCA of the codon usage frequencies of the promA plasmids. PromA  $\delta$   
806 plasmids are separated by the first dimension from the other plasmids, and PromA  $\beta$   
807 plasmids by the second dimension

808 **FIGURE 4** The *IS1071* insertion sites on various PromA  $\gamma$  plasmids. The residues  
809 between the *IS1071* transposon were deleted for simplicity, except the immediate  
810 flanking genes. The insertion locus of the pEN1 *IS1071* was marked on pPBL-H6-2  
811 with a triangle, and is conserved in other PromA- $\gamma$  plasmids. The slanted black lines on  
812 the *IS1071* ORF indicate immature stop codons. The *IS1071*-flanking backbone genes  
813 are numbered 1-4:

814 (1) *repB* (2) *mobA* (3) *trbM* (4) *VirD2*.

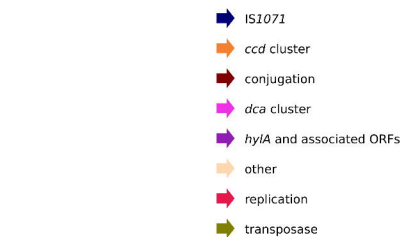
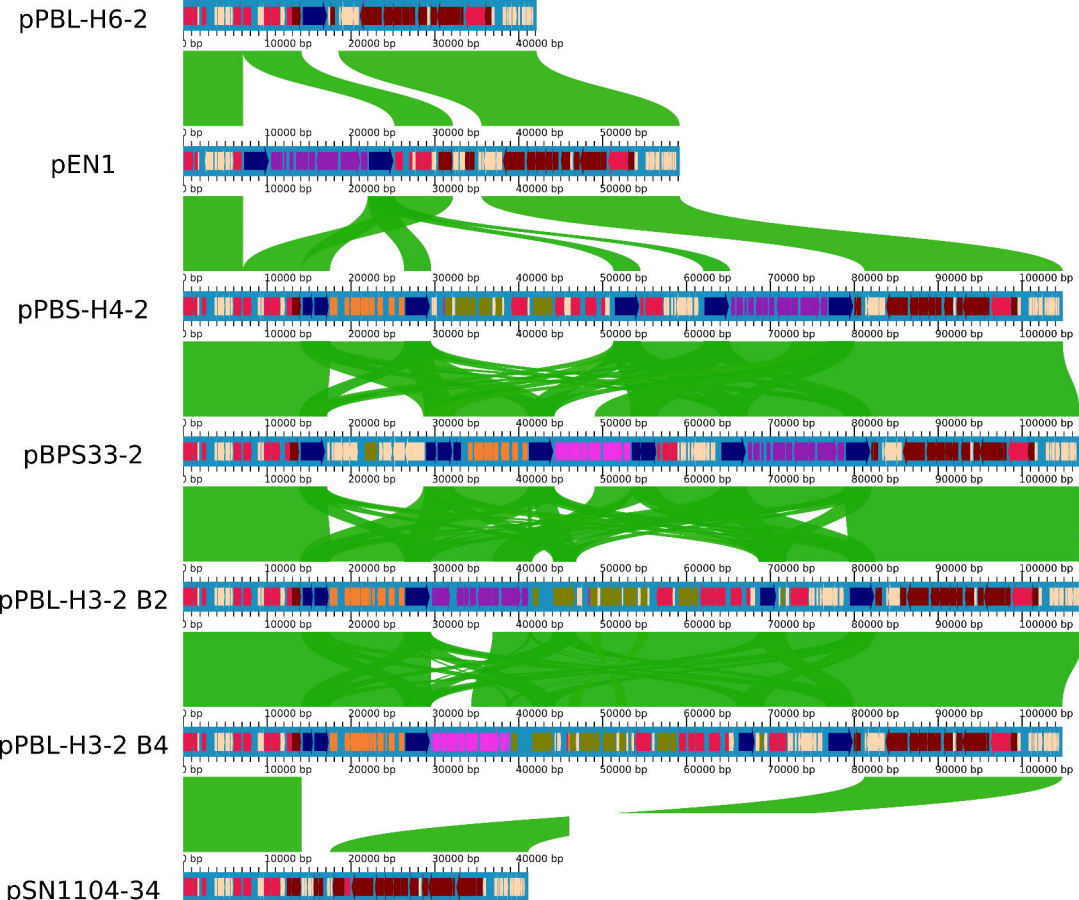
815 **FIGURE 5** Phylogeny of Hydrogenophaga species with fully-sequenced based on  
816 genomes on (a) whole genome sequences and (b) 16S rRNA gene sequences. The  
817 linuron-degrading Hydrogenophaga sp. PBL-H3 and BPS33 sequenced in this study  
818 are marked in bold. The branch lengths are scaled in terms of GBDP distance  
819 formula d5. The numbers above branches are GBDP pseudo-bootstrap support

820 values > 60% from 100 replications.

821 **Table 1. Statistics of the genomes and plasmids sequenced in this study**

	contig size	#CDS	%GC	# rRNA operons	#tRNA	classification
pEN1	59 kbp	68	63.4			PromA plasmid
<i>chr</i> BPS33	6.33 Mbp	5,830	65.7	2	53	chromosome
pBPS33-1	340 kbp	323	61.2			unclassified plasmid
pBPS33-2	107 kbp	109	63.1			PromA plasmid
<i>chr</i> PBL-H3	4.39 Mbp	4.39	65.6	2	44	chromosome
pPBL-H3-1	320 kbp	320	61.1			unclassified plasmid
pPBL-H3-2	107 kbp	107	62.8		1	PromA plasmid

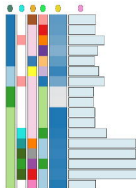
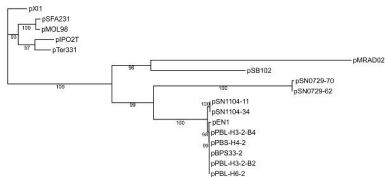
822

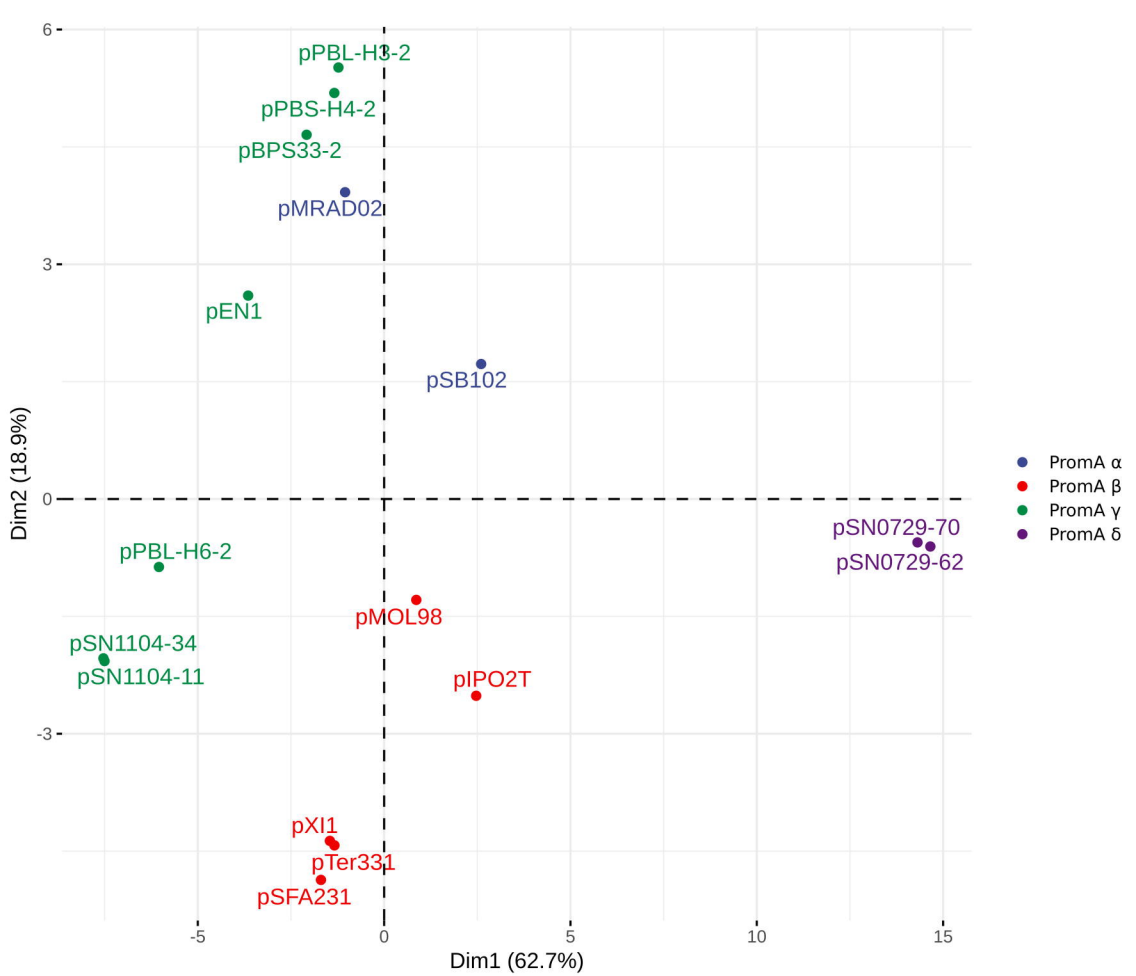


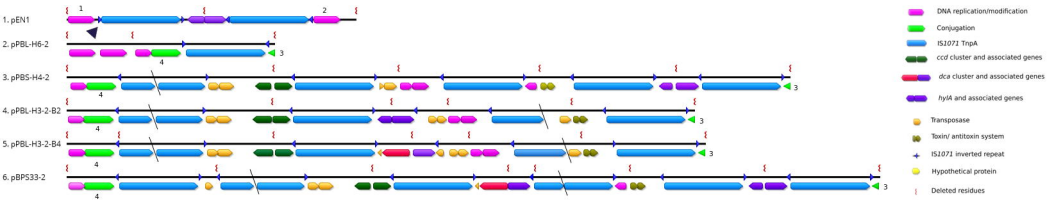




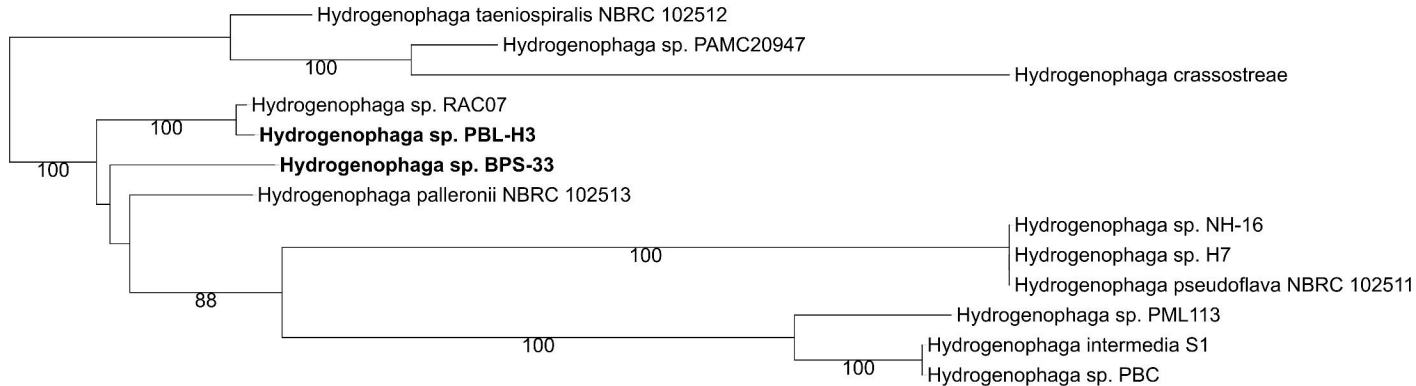
Tree scale: 0.1







Tree scale: 0.001



Tree scale: 0.01

